10 The weak interaction

10.1 General properties

In contrast with electromagnetic forces, the weak forces of nuclear physics are of short range, certainly less than nuclear dimensions, and are therefore not apparent as a property of matter in bulk. Recognition of the weak interaction as a fundamental natural process, therefore, had to await the advent of nuclear physics, but could, in principle, have been made at the very beginning, since the radiations observed in 1896 by becquerel are now known to be essentially due to the weak decay of daughter products of the uranium nucleus.

The phenomena now classed as weak are the non-electromagnetic decay processes and interactions that proceed on a time scale slow compared with a typical 'nuclear' time, say $R/c \approx 10^{-21}$ s where R is a nuclear radius. They may be grouped into:

(*a*) Purely leptonic processes, e.g. muon decay

$$\mu^+ \rightarrow e^+ + \nu_e + \bar{\nu}_\mu \qquad (t_{1/2} = 1{\cdot}5\ \mu\text{s},\ Q = 105\ \text{MeV}) \tag{10.1}$$

(*b*) Semi-leptonic processes, e.g. nuclear beta-decay

$$^{24}\text{Na} \rightarrow {}^{24}\text{Mg} + e^- + \bar{\nu}_e \qquad (t_{1/2} = 15{\cdot}4\ \text{h},\ Q = 5{\cdot}51\ \text{MeV}) \tag{10.2}$$

This category also includes atomic electron capture processes such as

$$^{7}\text{Be} + e^- \rightarrow {}^{7}\text{Li} + \nu_e \qquad (t_{1/2} = 53{\cdot}4\ \text{d},\ Q = 0{\cdot}86\ \text{MeV}) \tag{10.3}$$

and the analogous capture of muons in muonic atoms (Sect. 3.3)

$$^{12}\text{C} + \mu^- \rightarrow {}^{12}\text{B} + \nu_\mu \qquad (t_{1/2} \approx 1{\cdot}4 \times 10^{-6}\ \text{s},\ Q = 92\ \text{MeV}) \tag{10.4}$$

(*c*) Non-leptonic decays of strange particles, e.g.

$$K^0 \rightarrow \pi^+ + \pi^- \qquad (t_{1/2} \approx 10^{-8}\ \text{s},\ Q = 218\ \text{MeV}) \tag{10.5}$$

Experimental study of these processes has revealed new and basic properties of nature. First came the hypothesis of the neutrino; later, in a fruitful juxtaposition of events in nuclear and particle physics, the discovery of parity non-conservation in weak processes. There also came the important hypothesis of the non-conservation of strangeness in non-leptonic weak processes such as (10.5) and the recognition of the violation of other symmetries in kaon decay. More recently, and likely to be of outstanding importance for theoretical physics, are the discovery of neutral currents (Sect. 2.2.3) and the theories of Salam and Weinberg that unify the weak and the electromagnetic interactions.

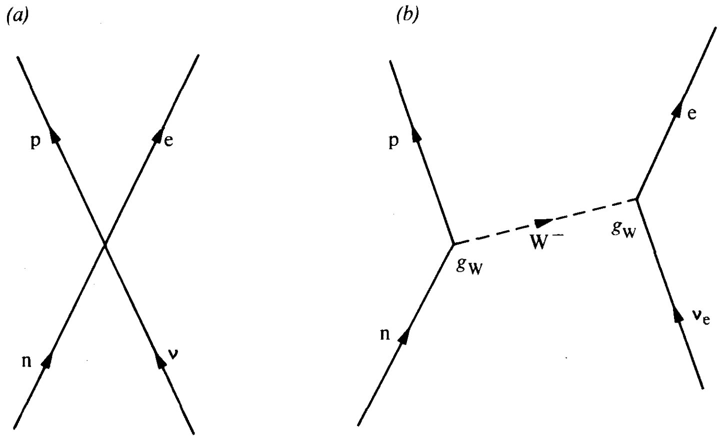

Fig. 10.1 The weak interaction. (*a*) Four-fermion point interaction, representing the beta decay of the neutron with absorption of a neutrino. (*b*) Beta decay of the neutron with an interaction of finite range, associated with exchange of a boson W^-.

In processes such as (10.2), (10.3) and (10.4) the weak interaction converts a bound neutron into a bound proton or vice versa; the *free* neutron decays to a proton in an exactly similar way

$$n \to p + e^- + \bar{\nu}_e \qquad (t_{1/2} = 10{\cdot}8\ \text{min},\ Q = 0{\cdot}782\ \text{MeV}) \tag{10.6a}$$

This decay may be written more symmetrically by replacing the antineutrino *emission* by neutrino *absorption*, to which it is equivalent:

$$n + \nu_e \to p + e^- \tag{10.6b}$$

Also, in processes such as (10.5), it is possible to introduce a virtual intermediate state in which a Λ-particle, a nucleon and a nucleon–antinucleon pair are present. It is thus possible to postulate that all weak interactions involve a four-fermion vertex, drawn for β-decay in Fig. 10.1*a*. If, however, the interaction is transmitted by an intermediate particle W the diagram is spread out (Fig. 10.1*b*) and then resembles the general interaction diagram drawn in Fig. 2.8. The strength of the weak interaction is represented by the magnitude g_W of the 'weak charge' associated with the vertices in Fig. 10.1*b*, but the intermediate particle W is not yet known experimentally, and until its mass M_W can be ascertained only a quantity proportional to g_W^2/M_W^2 can be determined by experiment. This quantity is known as the *weak interaction coupling constant* g and is analogous to the electromagnetic coupling constant $\alpha = (\mu_0 c^2/4\pi)e^2/\hbar c$. When expressed suitably in dimensionless form, the observed value of g is about $10^{-3}\alpha$. The theories that unify the weak and electromagnetic interactions predict a simple numerical relation between e and g_W that implies a boson mass $M_W \approx 40 m_p$.

10.2 Nuclear beta decay and lepton capture

10.2.1 Experimental information

Figure 9.7, which was presented in Section 9.3 in connection with the discussion of internal conversion, shows the spectrum of electron energies in the decay of 30-year ^{137}Cs, observed as a function of momentum p ($\propto B\rho$) in a magnetic spectrometer. If the contributions to the counting rate due to the sharp conversion lines are removed, the remaining electron spectrum is as shown in Fig. 10.2*a*. This continuous distribution, with an upper limit, is the beta-particle spectrum of the ^{137}Cs nucleus, whose main decay may be written

$$^{137}\text{Cs} \rightarrow {}^{137}\text{Ba}^* + \text{e}^- + \bar{\nu} \qquad (t_{1/2} = 30\ \text{a},\ Q = 0{\cdot}512\ \text{MeV}) \quad (10.7)$$

Because of the particular angular momenta involved, the main beta decay of ^{137}Cs is to an excited state of the residual nucleus but there is also a weak ground-state decay that contributes electrons to the spectrum; these have also been removed in Fig. 10.2*a*.

The main characteristics of a beta-decay process, which are obtained by experiment and are to be elucidated by theory are, for both electron and positron emitters:

(*a*) *The lifetime*, as mean life τ or halflife $t_{1/2}$, which ranges from a fraction of a second to 10^6 a and is 30 a in the ^{137}Cs example.

(*b*) *The maximum electron or positron energy* in the decay, given by the upper limit of the spectrum. This is not accurately obtainable from the direct spectrum, Fig. 10.2*a*, but by use of a theoretical factor (Sect. 10.2.3) a linear plot known as the *Fermi–Kurie plot* (see Ex. 10.9) may be obtained. This extrapolates to the upper limit (Fig. 10.2*b*) and may be used to deduce the Q_β value for the decay. This in turn, together with the energy of any associated γ-radiation such as the 662 keV transition in ^{137}Ba, can be used to connect the masses of the initial

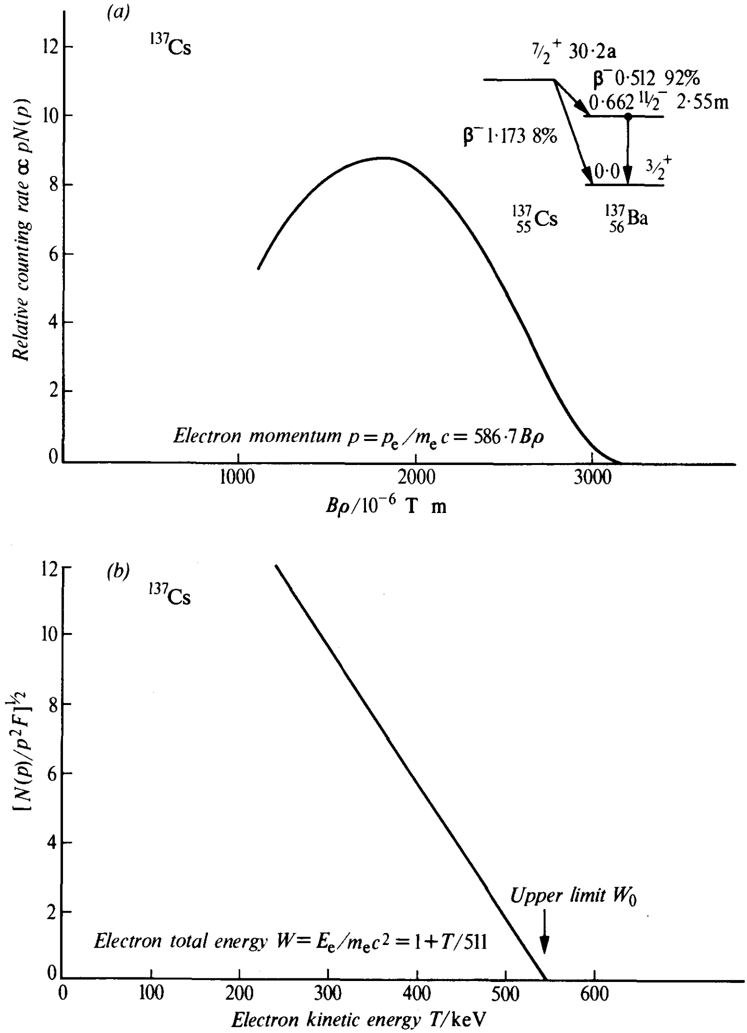

Fig. 10.2 The beta spectrum. (*a*) Sketch of electron distribution for ^{137}Cs obtained from Fig. 9.7 by removing internal conversion lines and the yield due to the high-energy transition. The ordinate is the counting rate at a spectrometer setting p, which is proportional to $pN(p)$ where $N(p)$ is the number of decay electrons per unit momentum at momentum p. (*b*) Fermi–Kurie plot to determine the end point of the spectrum. The abscissa gives electron kinetic energy (= electron total energy $-m_ec^2$). The ^{137}Cs decay is first-forbidden, and the FK plot in an accurate experiment is actually curved because of an energy-dependent shape factor additional to the Fermi factor F used in the ordinate. Omission of this factor means that an accurate end-point energy is not expected in the present case.

and final nuclei, on the assumption of zero mass for the neutrino. It is often convenient to express the upper limit in terms of the *total* electron energy, i.e. including mass-energy $m_e c^2$ and it is then written E_0, or in units of $m_e c^2$, W_0 $(=E_0/m_e c^2)$.

(*c*) *The detailed shape* of the electron or positron spectrum as a function of total energy E_e $(W = E_e/m_e c^2)$ or momentum p_e $(p = p_e/m_e c)$.

This information permits a broad classification of β-emitting bodies and often gives an indication of spin and parity changes in the decay. In addition, in recent years, and because of interest in the fundamental nature of the weak interaction, there has been much work on:

(*d*) The correlation between the spatial and spin directions of the particles concerned in the decay (Sect. 10.4.2).

10.2.2 *Classification*

The extensive range of nuclear beta-decay lifetimes may be roughly ordered by calculating a quantity known as the *comparative halflife* $ft_{1/2}$ (often called the ft-value). The numerical factor f (Sect. 10.2.3, eqn (10.21)) is determined mainly by the energy release E_0 in the decay, and is strongly dependent on this quantity ($\approx E_0^5$ for high energies). Use of $ft_{1/2}$ values rather than $t_{1/2}$ leads directly to the basic quantity $1/(g^2\,|M|^2)$ where g is the weak interaction coupling constant and M is the nuclear matrix element. The number distribution for odd-mass beta-decaying nuclei with respect to $\log ft_{1/2}$ is shown in Fig. 10.3.

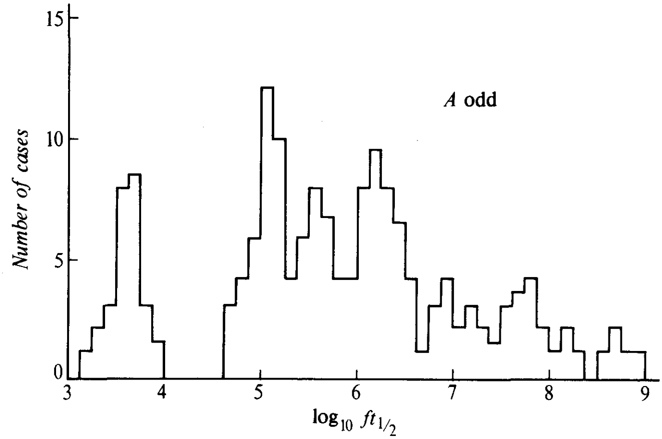

Fig 10.3 Comparative halflife for beta transitions between ground states of odd-mass nuclei (Feenberg, E. and Trigg, G., *Rev. Mod. Phys.*, **22,** 399, 1950).

A group in the distribution shown in the figure suggests that for the corresponding decays the nuclear matrix element is independent of Z and of W_0. A clear case arises for $\log ft_{1/2} \approx 3$–4 which relates to especially probable transitions known as *superallowed*, in which it seems likely that there is excellent overlap between the initial and final nucleon wavefunctions. Decays of mirror nuclei (e.g. $^{13}N \rightarrow {}^{13}C$) and decays within isobaric triplets (e.g. $^{26}Si \rightarrow {}^{26}Al \rightarrow {}^{26}Mg$) fall into this class.

Other groupings perhaps exist for $\log ft_{1/2} \approx 4$–5 and for $\log ft_{1/2} > 6$. For the former, the transitions may be *allowed* in the sense of the selection rules (Sect. 10.2.4) but are unfavoured with respect to the superallowed group because of change of nucleon wavefunction. The latter are the *forbidden transitions*, in which there is a more drastic change of structure. It will be seen in Section 10.2.3 that the $ft_{1/2}$ classification can equally well be described in terms of the orbital angular momentum transported by the leptons in the decay.

10.2.3 The neutrino and the Fermi theory

The starting point of the Fermi theory of beta decay is the Pauli hypothesis of the neutrino, a massless fermion that is created together with an electron in the beta-decay process just as a photon is created in a radiative transition between nuclear levels, but of course with a different probability. At the present point, neutrino is taken to embrace antineutrino and electron to include positron.

The neutrino was required because beta decay connects nuclear states with definite energy, angular momentum and parity. The continuous nature of the beta energy distribution (Fig. 10.2*a*) and the fact that no other familiar type of radiation could be seen in beta-decay processes (excepting, of course, radiation from the residual nucleus) meant that some new means of restoring an energy balance was required. Equally, it was necessary to ensure a similar balance of linear momentum in the decay. Moreover, since beta decay does not change mass number the initial and final nuclei must either both have integral or both have half-integral spin and the emission of only one fermion between these two states cannot conserve angular momentum.

Long after Pauli's hypothesis, the discovery of parity non-conservation in weak interactions (Sect. 10.4.2) led to the recognition of a specific connection between the momentum and spin vectors for a neutrino analogous to the circular polarization of a light quantum, but differing from it in that only one sense is permitted. For a massless fermion, it is useful to describe this property as *helicity*, and to speak of helicity states $+1$ and -1 corresponding with spin parallel or antiparallel with the direction of motion. If this is included, the properties required for the neutrino in a typical decay process are:

(*a*) zero charge;
(*b*) zero mass, since all experiments confirm the conclusion that the upper limit of the beta spectrum gives the energy change in the decay;
(*c*) half-integral angular momentum;
(*d*) extremely small interaction with matter because of the failure of conventional experiments to detect neutrino ionization;
(*e*) unit helicity ($\mathcal{H} = \pm 1$). This implies (*b*) and (*c*), i.e. that the neutrino is a massless fermion and consequently that it has a distinct *antiparticle*, the antineutrino $\bar{\nu}$, with opposite helicity.

The neutrino differs from a light quantum in respects (*c*) and (*d*) and in the fact that it is not associated with an electromagnetic field. It is, as shown in Fig. 10.1*a*, *not* the exchange particle of the weak interaction. Direct experimental evidence for the existence of the neutrino, apart from its success in making possible a theory of beta decay, is reviewed in Section 10.4.2.

The probability per unit time of a beta-decay process

$$(A, Z) \rightarrow (A, Z \pm 1) + \mathrm{e} + \nu \tag{10.8}$$

releasing total energy $E_0 = E_\mathrm{e} + E_\nu$ is given by time-dependent perturbation theory as

$$T_{if} = (2\pi/\hbar)\,|H_{if}|^2\,\rho(E) = \lambda, \quad \text{say} \tag{10.9}$$

where H_{if} is the matrix element of the weak interaction Hamiltonian operator H_β between initial and final states i, f, and $\rho(E)$ is the number of momentum states in the volume V of the final system per unit energy at the total energy $E = E_0$. The hadronic wavefunctions to be used in the matrix element H_{if} are those of the initial and final nuclei, so that beta decay is basically a many-body problem. It is, however, possible to divide the calculation into a summation over single-particle transitions $\mathrm{n} \overset{\beta,\nu}{\rightleftarrows} \mathrm{p}$, plus small corrections due to many-body features. The latter will not be considered here; a discussion of such features will be found in Reference 11.4.

In its simplest version the theory of beta decay expresses a nucleon transition in the process (10.8) in the symmetrical form of equation (10.6b) in which two particles are absorbed and two created. The interaction Hamiltonian H_β cannot be given a specific form, as in the case of the electromagnetic interaction, but it clearly produces both a hadronic (nucleon) transition and the emission of leptons. If we indicate these processes by dimensionless operators $\boldsymbol{O}_h$ and $\boldsymbol{O}_l$ respectively then a possible form for the decay is

$$H_\beta = g\boldsymbol{O}_h[\phi_\mathrm{e}^* \boldsymbol{O}_l \phi_\nu] \tag{10.10}$$

where g is a coupling constant. The matrix element between initial and final nucleon states is then

$$H_{if} = g\int (\psi_f^* \boldsymbol{O}_h \psi_i)(\phi_e^* \boldsymbol{O}_l \phi_\nu)\, d^3\boldsymbol{r} \tag{10.11}$$

in which it is assumed that all the particles interact at a point. As in the electromagnetic case we also assume a normalization of wavefunctions such that the system volume V does not appear in T_{if}. If the matrix element is to be an energy the coupling constant g then has the dimensions energy × volume.

The nature of the operators $\boldsymbol{O}_h$ and $\boldsymbol{O}_l$ will be discussed in Section 10.4. For the present, we recall that the vector potential in the electromagnetic interaction could be written as an outgoing plane wave and note that in the nucleon weak decay there are lepton waves in the final state (10.6a) or in both initial and final state (10.6b). Assuming again a plane wave system and omitting the $e^{i\omega t}$ term, these waves contribute a factor $e^{i\boldsymbol{k}.\boldsymbol{r}}$ to the matrix element, where $\boldsymbol{k} = \boldsymbol{k}_e + \boldsymbol{k}_\nu$ is the sum of the electron and neutrino wave vectors. For $\boldsymbol{r} \approx \boldsymbol{R}$, the nuclear radius, $\boldsymbol{k}\cdot\boldsymbol{r}$ is normally small ($\approx 0{\cdot}1$) and an expansion of the exponential may be made, either directly or in multipoles. Successive terms in this expansion correspond with the emission of the electron–neutrino pair in (10.8) with $l = 0, 1, 2, \ldots$ units of *orbital* angular momentum; strictly, it is not possible to separate orbital from total angular momentum for relativistic fermions but here a non-relativistic treatment is used. The transition probability associated with these terms decreases as $(kR)^2$ as l increases and this offers an explanation of the empirical classification of beta-decay processes into allowed ($l = 0$) and forbidden ($l \geqslant 1$) types. If the factor r^l is taken from the expansion into the interaction operator, leaving energy-dependent factors outside it, the classification is then related to the nuclear matrix element of the weak interaction and selection rules (Sect. 10.2.4) for changes of nuclear spin and parity may be inferred, as in the electromagnetic case.

We now consider specifically an *allowed transition* ($l = 0$), i.e. s-wave lepton emission. We replace the lepton bracket in (10.11) by unity although the operator $\boldsymbol{O}_l$ must still be considered to determine the fundamental nature of the lepton emission, as discussed in Section 10.4. The operator $\boldsymbol{O}_h$ could be simply the isospin-shifting operator τ^+ that converts a neutron into a proton. The matrix element for the transition (I_i, m_i) to (I_f, m_f) then reduces to

$$H_{if} = g\int \psi_f^* \tau^+ \psi_i \, d^3\boldsymbol{r} \tag{10.12}$$

If this is summed for all nucleons the isospin factor becomes T^+ and if the squared matrix element is averaged over the initial substates and summed over the final substates, allowing for lepton spins, we obtain the squared *nuclear matrix element* $|M|^2 = |H_{if}|^2/g^2$.

The density of states factor $\rho(E)$ in (10.9) refers to all possible distributions of energy between the electron and the neutrino and to a total energy E_0 within a range of width dE_0. For each electron energy E_e, the neutrino energy E_ν is $E_0 - E_e$ because the heavy recoil nucleus $(A, Z \pm 1)$ to which the nucleon is bound takes very little energy. The nucleus does, however, participate in the momentum balance so that the direction of the neutrino momentum is not determined by that of the electron. The factor $\rho(E)$ is, therefore, a product of phase-space factors for both electron and neutrino but with no statistical weight $2s+1$ for intrinsic spins since this is implicit in the overall squared matrix element. For lepton momenta p_e, p_ν the transition probability for the selected energy range may therefore be written, omitting volume factors,

$$d\lambda = (2\pi/\hbar)g^2\,|M|^2 \cdot \frac{4\pi p_e^2\,dp_e}{h^3} \cdot \frac{4\pi p_\nu^2\,dp_\nu}{h^3} \cdot \frac{1}{dE_0} \tag{10.13}$$

using the standard form $4\pi p^2\,dp/h^3$ for the number of states per unit volume at momentum p. Remembering that for the leptons, assuming a finite neutrino mass m_ν,

$$\left.\begin{aligned} E_e^2 &= p_e^2c^2 + m_e^2c^4 \\ E_\nu^2 &= p_\nu^2c^2 + m_\nu^2c^4 \end{aligned}\right\} \tag{10.14}$$

we have

$$\left.\begin{aligned} c^2p_e\,dp_e &= E_e\,dE_e \\ c^2p_\nu\,dp_\nu &= E_\nu\,dE_\nu \end{aligned}\right\} \tag{10.15}$$

Also, for a given electron energy $dE_\nu = dE_0$, so that (10.13) becomes

$$d\lambda = (1/2\pi^3)(g^2\,|M|^2/\hbar^7c^4)p_ep_\nu E_eE_\nu\,dE_e \tag{10.16}$$

Equation (10.16) gives the energy distribution in the beta spectrum; for $m_\nu = m_e$ it would be symmetrical about the mean energy in the absence of Coulomb effects, but for $m_\nu = 0$ the maximum yield is shifted to a lower energy.

If the dimensionless variables W and p are used instead of E_e and p_e for the electron total energy and momentum, and if m_ν is set equal to zero, equation (10.16) becomes

$$d\lambda = (1/2\pi^3)(g^2\,|M|^2\,m_e^5c^4/\hbar)pW(W_0 - W)^2\,dW \tag{10.17}$$

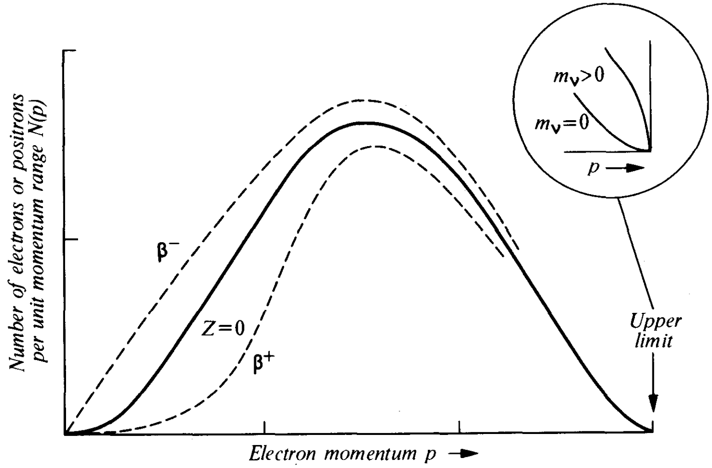

Fig 10.4 The beta spectrum. The full line marked $Z=0$ shows the momentum distribution in beta decay without Coulomb correction. Introduction of the Fermi factor alters the statistical shape as shown schematically by the dotted lines for electrons and positrons. The inset is an enlarged version of the spectrum near the upper limit in the cases of zero and finite neutrino mass.

or, in terms of momenta rather than energies,

$$d\lambda = (1/2\pi^3)(g^2\,|M|^2\,m_e^5c^4/\hbar^7)p^2(W_0-W)^2\,dp \qquad (10.18)$$

The momentum distribution $N(p)=d\lambda/dp$ is plotted in Fig. 10.4. This spectrum approaches zero intensity at the upper limit with a horizontal tangent if $m_\nu=0$ but with a vertical tangent if m_ν is finite as shown in the figure inset. Detailed experimental study of the spectrum for the tritium decay $^3H\rightarrow{}^3He+e^-+\bar{\nu}$ near the upper limit has set the present upper bound $m_\nu<(1/8500)m_e$, i.e. <60 eV.

If the nuclear matrix element is energy-independent it follows from (10.18) that if the number of electrons per unit momentum range in the spectrum $N(p)=d\lambda/dp$ is plotted as $[N(p)/p^2]^{1/2}$ against W, the graph should extrapolate to the total energy W_0 corresponding to the upper limit. This, however, is not precise enough because all electron and positron distributions are affected by the nuclear charge and the calculable Fermi factor $F(Z\pm1,p)$ must be introduced to correct for this. The plot of $[N(p)/p^2F]^{1/2}$ against W is the Fermi–Kurie plot, shown for ^{137}Cs in Fig. 10.2*b*. The factor F is really a penetration factor for the nuclear Coulomb barrier; its effect is to suppress low energies in positron spectra and to enhance them in the case of electrons; the spectral shape then changes as indicated by the dotted lines in Fig. 10.4.

The total decay probability λ for the transition (10.8) may now be obtained as

$$\lambda = \int d\lambda = (1/2\pi^3)(g^2\,|M|^2\,c^4 m_e^5/\hbar^7) \times \int_0^{p_0} p^2 F(Z\pm 1, p)(W_0 - W)^2\,dp \quad (10.19)$$

where p_0 is the electron momentum corresponding to the upper limit of the spectrum. This is normally written in terms of the halflife $t_{1/2}$ for the decay

$$(\ln 2)/t_{1/2} = (1/2\pi^3)(g^2\,|M|\,c^4 m_e^5/\hbar^7) f(Z\pm 1, p_0) \quad (10.20)$$

where

$$f(Z\pm 1, p_0) = \int_0^{p_0} p^2 F(Z\pm 1, p)(W_0 - W)^2\,dp \quad (10.21a)$$

$$= \int_1^{W_0} pWF(Z\pm 1, W)(W_0 - W)^2\,dW \quad (10.21b)$$

may be derived from tabulated values of the Fermi function F, and W and p are related by the expression, given by (10.14) for E_e,

$$W^2 = 1 + p^2 \quad (10.22)$$

The quantity $ft_{1/2}$ obtained from (10.20) is the comparative halflife (Sect. 10.2.2) for allowed decays, in which the leptons remove zero orbital angular momentum. Within the allowed class, groupings correspond to particular values of the structure-dependent nuclear matrix element M. If this quantity is known, as it is for some of the simplest nuclei, the $ft_{1/2}$-value yields the coupling constant g; this is found to be $1{\cdot}41 \times 10^{-62}$ J m^3 (Sect. 10.4.3).

The Fermi theory is immediately applicable to the nuclear capture of electrons or negative muons from an atomic orbit, processes (10.3) and (10.4). Only *two* particles are then involved in the actual final state, the residual nucleus and the neutrino, and the latter essentially has a unique energy if only one final nuclear state is involved. The capture probability is directly predictable from (10.9) using the $\rho(E)$ appropriate to a two-body final state and an initial lepton wavefunction representing a particle bound in the *original* atom rather than a plane wave. For an s-state, with Bohr radius a ($a_\mu = \frac{1}{207} a_e$) this is

$$\phi(r) = (1/\pi^{1/2})(Z/a)^{3/2} \exp(-Zr/a) \quad (10.23)$$

and the particle density at the nucleus is $|\phi(0)|^2$. The number of final neutrino states per unit energy range is as in (10.13) with $dE_0 = dE_\nu$

$$\rho(E) = \frac{4\pi p_\nu^2\,dp_\nu}{h^3} \cdot \frac{1}{dE_0} = \frac{4\pi p_\nu^2}{h^3 c} \quad (10.24)$$

For electron capture, the stability conditions, equation (6.24), show that the overall energy release is just $m_e c^2$ (511 keV) greater than the *total* energy $W_0 m_e c^2$ available for the alternative process of positron decay between the same initial and final nuclei, neglecting nuclear recoil and atomic binding energy terms.

For an allowed nuclear transition, we obtain from (10.9), (10.23) and (10.24) the probability of electron capture averaged over the K-electrons as

$$\lambda_K = (1/2\pi^3)(g^2 |M|^2 m_e^2 c/\hbar^4)(Z/a)^3 2\pi(W_0+1)^2 \qquad (10.25)$$

and in the present approximation the ratio of the intensity of this transition λ_K to that of positron emission, λ_+, does not depend on the nuclear matrix element.

In some cases, e.g. $^7Be \rightarrow {}^7Li$ (eqn (10.3)) insufficient energy is available for positron decay and electron capture is the only decay mode. Generally, because of the additional energy available, the increased density of atomic electrons near the nucleus for heavy atoms, and the deterrent effect of the nuclear potential barrier on low-energy positron emission, electron capture increases in relative importance with Z. Capture is usually observed by detection of X-rays from the atomic vacancy; the decay constant λ_K can be altered by about 0·01 per cent by altering the electronic environment of the nucleus by chemical methods.

Muon capture, such as that shown in equation (10.4), may take place from the K-shell of a muonic atom. The basic process is

$$\mu^- + p \rightarrow n + \nu_\mu \qquad (10.26)$$

and this releases an energy of about 106 MeV so that many nuclear states may be excited. Gamma radiation from these states may be detected. Since the muon has to find a proton with which to interact, the capture probability includes an extra factor Z in comparison with electron-capture, i.e. $\lambda_{\mu c} \propto Z^4$. In practice, decay of the muon is more probable for $Z \approx 10$ or less. The intrinsic probability is still determined by the weak interaction coupling constant, but additional nuclear matrix elements are now important because of the high momentum transfer.

10.2.4 *Selection rules* (*non-relativistic*)

Among the most probable beta decays, namely the *superallowed* transitions with $ft_{1/2} \approx 3100$ s, are found the transitions

$$^{14}O \rightarrow {}^{14}N^* + e^+ + \nu \qquad (10.27)$$

in which the nuclear spin change is from 0^+ to 0^+, and

$$^6He \rightarrow {}^6Li + e^- + \bar{\nu} \qquad (10.28)$$

in which the spin change is from 0^+ to 1^+.

In the non-relativistic approximation used hitherto, which of course cannot be generally accurate for electron + neutrino emission, orbital and spin angular momenta have been considered separately. If the allowed character of (10.27) and (10.28) is attributed to s-wave emission of the lepton pair the total angular momentum change must be provided by appropriate alignment of the two lepton spins of $\frac{1}{2}\hbar$. In cases such as (10.27) with $\Delta I = 0$ the electron and neutrino are emitted with spins antiparallel; these are known as *Fermi transitions* (F). For decays such as (10.28) with $\Delta I = 1$ the lepton spins are parallel and these are *Gamow–Teller transitions* (GT).

Evidently the nuclear matrix elements for F and GT transitions will be different and in decays in which both types of transition are possible, e.g. for spin changes $\frac{1}{2}^{\pm} \to \frac{1}{2}^{\pm}$ or $1^{\pm} \to 1^{\pm}$ the matrix element is written

$$|M|^2 = C_F^2 |M_F|^2 + C_{GT}^2 |M_{GT}|^2 \qquad (10.29a)$$

where C_F and C_{GT} are coupling constants in units of g. The ratio $|C_{GT}/C_F|^2$ depends on the weak interaction itself. The ratio $|M_{GT}/M_F|^2$ is dependent on nuclear structure and can be predicted accurately only in simple cases, e.g. neutron decay. In the next section, evidence will be presented for the identification of C_F and C_{GT} with the vector (V) and axial vector (A) coupling constants C_V and C_A and if we write $g_V = gC_V$ and $g_A = gC_A$ then equation (10.20) takes the general form (after some rearrangement).

$$ft_{1/2} = \frac{K}{g_V^2 |M_F|^2 + g_A^2 |M_{GT}|^2} \qquad (10.29b)$$

where K is known, from the values of the fundamental constants appearing in equation (10.20), to be $1{\cdot}2308 \times 10^{-120}\ \mathrm{J^2\,m^6\,s}$.

The two types of transition are clearly also possible in forbidden decays, as shown in the non-relativistic selection rules given in Table 10.1. These results apply to spin and parity changes for the initial and final nuclear states, for which isobaric spin is a good quantum number. The isospins actually observed show that this quantity is

TABLE 10.1 Selection rules for beta decay (non-relativistic)

Type of transition	*Fermi*		*Gamow–Teller*	
	Spin ch.	*Parity ch.*	*Spin ch.*	*Parity ch.*
Allowed	0	No	0 (except 0→0), ±1	No
First forbidden	0 (except 0→0), ±1	Yes	0, ±1, ±2	Yes

not conserved in the weak interaction, since allowed transitions with $\Delta T=0, \pm 1$ are found. In the Fermi superallowed decays, identity of initial and final state wavefunctions implies $\Delta T=0$ and since there must be at least two nuclei related by the transition, $T \geqslant \frac{1}{2}$. If $\Delta T \neq 0$, Fermi transitions are *isospin-forbidden* and then take place, with reduced probability, because of isospin impurities in the initial and final states.

10.3 Muon decay

Figure 10.5*a* is a spectrum of the electrons observed from the decay of muons at rest, process (10.1). The spectrum is continuous, suggesting that the final state contains three particles and it tends to a maximum intensity at the upper limit, suggesting that two particles can emerge directly opposite to the decay electron with high probability, as shown in Fig. 10.5*b*. The maximum electron energy is $\approx 54\,\text{MeV}$, i.e. about half the muon mass, and no high-energy radiation is observed so that processes such as $\mu \rightarrow e+\gamma$ and $\mu \rightarrow e+2\gamma$ are ruled out.

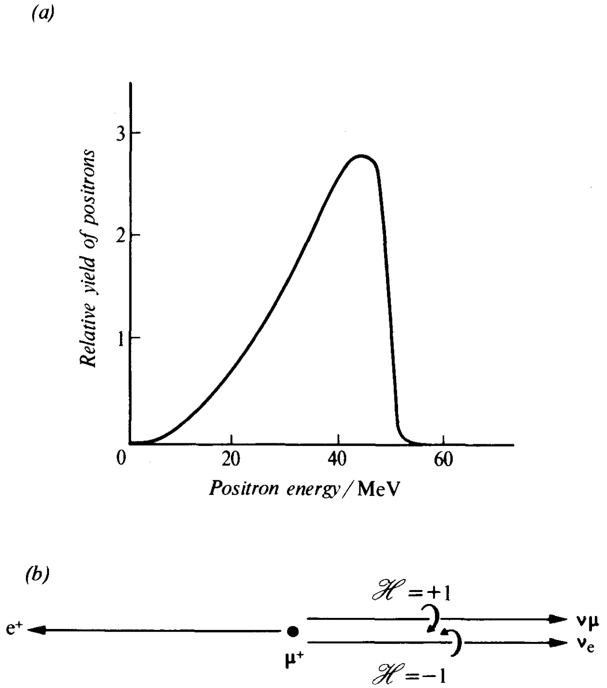

Fig. 10.5 Muon decay. (*a*) Spectrum of positrons from decay of a μ^+-particle at rest. (*b*) Helicities of neutrinos in μ^+-decay. (Note: ν_μ should read $\bar{\nu}_\mu$)

The purely leptonic processes that account for these facts are, as already indicated for μ^+ in (10.1),

$$\begin{aligned}\mu^- &\rightarrow e^- + \bar{\nu}_e + \nu_\mu \\ \mu^+ &\rightarrow e^+ + \nu_e + \bar{\nu}_\mu\end{aligned} \tag{10.30}$$

Figure 10.5*b* shows that the two neutrinos emitted cannot be identical because these particles have a definite helicity and the highly probable collinear decay then implies that two identical fermions are emitted in the same state of motion. This is forbidden by the Pauli principle, and for identical neutrinos the electron intensity would tend to zero at the upper limit. It was originally thought that the neutrinos might be particle and antiparticle, but it is now known that there is an additional difference, namely that, as shown above, one is electron-associated and the other muon-associated. The form in which the processes (10.30) is written implies a law of lepton conservation for both (e, ν_e) and (μ, ν_μ) with μ^-, e^- counted as particles and μ^+, e^+ as antiparticles.

The fact that there are two distinct kinds of neutrino in nature, each with its own antiparticle, was established by experiments in which neutrinos from pion decay

$$\pi \rightarrow \mu + \nu \tag{10.31}$$

were allowed to pass through the plates of a large spark chamber. It was found that occasionally an interaction with a nuclear proton

$$\nu_\mu + p \rightarrow n + \mu \tag{10.32}$$

would produce a muon, but no electrons from the reaction

$$\nu_e + p \rightarrow n + e \tag{10.33}$$

were seen, although they have been expected to produce a very obvious electromagnetic shower in the spark chamber.

The neutrino ν_e has a mass <60 eV. The mass of the neutrino ν_μ is known with less precision but certainly seems to be <650 keV. If it is assumed that both particles have zero mass then the muon-to-electron decay probability may be calculated using perturbation theory. The result, which assumes also that all the fermions have unit helicity if fully relativistic, is that

$$\lambda_\mu = 1/\tau_\mu = g_\mu^2 m_\mu^5 c^4 / 192\pi^3 \hbar^7 \tag{10.34}$$

No nuclear matrix element, with attendant uncertainty of nuclear structure, appears in this expression, and since both the mean life of the free muon and its mass are known to high accuracy, the coupling constant g_μ may be obtained from these data with similar accuracy. Its value, after some small electromagnetic corrections, will be discussed in Section 10.4.3.

10.4 Nature of the weak interaction in nuclear beta decay

The discussion of beta processes in Section 10.3 was phenomenological and presented no detailed account of the weak interaction matrix element. Such an account was possible in the electromagnetic case because of the existence of a full classical theory in which an energy could arise from the interaction of a current density and a vector potential and, therefore, also from the interaction of two currents. Fermi's original formulation of weak interaction theory proceeded in close analogy with electromagnetic theory and leads, in fact, to a similar current–current type of interaction, although the charges concerned are the 'weak charges' g_W of Fig. 10.1*b* rather than the electric charges *e*, and the currents interact only over a very small region, perhaps only at a point, rather than over all space. In the present section an outline is given of the way in which this formulation leads to a matrix element, starting with appropriate wavefunctions for the leptons and hadrons concerned and appealing directly to experiment to select the combinations that actually occur in nature. A more detailed discussion will be found in Reference 1.1a, Chapter 4.

10.4.1 Relativistic invariants

Electromagnetic theory, as described by Maxwell's equations, is invariant under a Lorentz transformation and it is reasonable to expect that the beta-decay matrix element (squared) shall also be a Lorentz invariant. Of the four wavefunctions appearing in H_{if}, equation (10.11), ϕ_e and ϕ_ν are solutions of the Dirac equation for fermions of finite and zero mass respectively, while ψ_f and ψ_i are solutions of the Schrödinger equation since the nucleons are non-relativistic. No discussion of the Dirac equation will be given in this book except to note that for a given four-momentum the equation has four independent solutions (corresponding in the non-relativistic limit to a particle with spin up or spin down with positive or negative energy, i.e. to particle and antiparticle).

The leptonic wavefunctions ϕ, therefore, have *four components* and the weak interaction operator $\boldsymbol{O}_l$ assembles these into sums of products. It is found that these products can be arranged into one or more of five different forms having well-defined properties under a Lorentz transformation and listed below:

(*a*) a *scalar* (S);
(*b*) a *four-vector* (V);
(*c*) an *antisymmetric tensor* (T);
(*d*) an *axial vector* (A);
(*e*) a *pseudoscalar* (P).

The four-vector and tensor are analogous to the corresponding quantities in electromagnetic theory. An axial vector describes quantities such as angular momentum and a pseudoscalar is, for instance, the scalar product of an axial vector with a velocity. It therefore has the important property that it changes sign under the parity, or mirror reflection, operation.

If the matrix element (10.11) is to be an energy, i.e. a scalar, a simple prescription is to allow the operator $\boldsymbol{O}_l = \boldsymbol{O}$ to act on the nucleonic wavefunctions as it does on the leptonic functions. The matrix element may then be written

$$H_{if} = g\int (\psi_f^* \boldsymbol{O}\psi_i)(\phi_e^* \boldsymbol{O}\phi_\nu)\, \mathrm{d}^3 r \tag{10.35}$$

for a particular operator, and if all suitable operators are included

$$H_{if} = g\int \sum_x C_x (\psi_f^* \boldsymbol{O}_x\psi_i)(\phi_e^* \boldsymbol{O}_x\phi_\nu)\, \mathrm{d}^3 r \tag{10.36}$$

where $x =$ S, V, T, A, P and the C_x are coupling coefficients, in units of g.

10.4.2 Basic experiments on the interaction

Studies of decay rate and spectrum shape do not by themselves determine the precise nature of the weak interaction matrix element. They do, however, provide a starting point by establishing properties (a)–(d) of the associated neutrino, as listed in Section 10.2.3. The evidence that the neutrino and antineutrino of beta decay are distinct particles is the failure to observe the reaction

$${}^{37}_{17}\mathrm{Cl} + \bar{\nu}_e \rightarrow {}^{37}_{18}\mathrm{A} + \mathrm{e}^- \tag{10.37}$$

when antineutrinos from beta-decaying fission products in a nuclear reactor, e.g. reactions such as

$${}^{140}_{57}\mathrm{La} \rightarrow {}^{140}_{58}\mathrm{Ce} + \mathrm{e}^- + \bar{\nu}_e \tag{10.38}$$

are allowed to pass through a volume of chlorine. No radioactive ^{37}A decaying by the electron-capture process

$${}^{37}_{18}\mathrm{A} + \mathrm{e}^- \rightarrow {}^{37}_{17}\mathrm{Cl} + \nu_e \tag{10.39}$$

was found. This experimental result verifies that (10.37) and (10.39) are *not* equivalent forward and backward reactions as they would be if the neutrino and antineutrino were identical particles. The same conclusion follows from the fact that double beta-decay processes such as

$${}^{124}\mathrm{Sn} \rightarrow {}^{124}\mathrm{Te} + 2\mathrm{e}^- + 2\bar{\nu}_e \tag{10.40}$$

experimentally have a much lower probability than would be the case if the reaction could proceed in two stages

$$\left.\begin{array}{l} {}^{124}\mathrm{Sn} \rightarrow {}^{124}\mathrm{Sb} + \mathrm{e}^- + \bar{\nu}_\mathrm{e} \\ \bar{\nu}_\mathrm{e} + {}^{124}\mathrm{Sb} \rightarrow {}^{124}\mathrm{Te} + \mathrm{e}^- \end{array}\right\} \tag{10.41}$$

Lepton conservation, with distinct ν_e and $\bar{\nu}_\mathrm{e}$, requires that the second stage should involve absorption of a neutrino. On the other hand, and now in a positive sense, antineutrino absorption has been demonstrated by Reines and Cowan for the 'inverse β' process

$$\bar{\nu}_\mathrm{e} + \mathrm{p} \rightarrow \mathrm{n} + \mathrm{e}^+ \tag{10.42}$$

which is formally equivalent to the neutron decay

$$\mathrm{n} \rightarrow \mathrm{p} + \mathrm{e}^- + \bar{\nu}_\mathrm{e} \tag{10.43}$$

The absorption was indicated by the appearance of a prompt positron e^+, with associated annihilation quanta, followed by radiations from the capture of the thermalized neutron in cadmium present in the reaction vessel.

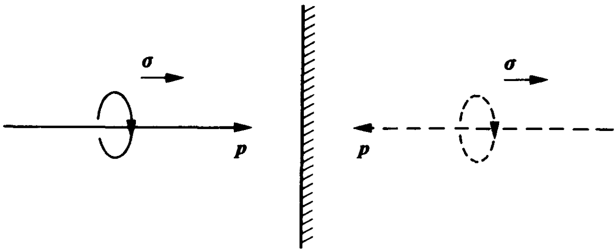

Fig. 10.6 Mirror reflection of a particle with definite helicity. The operation reverses the sign of the product $\boldsymbol{\sigma} \cdot \boldsymbol{p}$; the spin operator $\boldsymbol{\sigma}$ is used so that the eigenvalues of helicity are unity.

The property of helicity for the (zero-mass) neutrino was not acceptable while strict conservation of parity in the weak interaction was required. This may be seen in Fig. 10.6, which shows that the mirror reflection, to which the parity operation is equivalent, turns a right-handed ($\mathscr{H} = +1$) particle into a left-handed particle ($\mathscr{H} = -1$), e.g. $\bar{\nu} \rightarrow \nu$, so that the physical situation changes. The form of the weak interaction in beta-decay was studied before helicity considerations were recognized, by investigating the *correlation* between the direction of electron emission and of antineutrino emission in a suitable decay, such as ${}^6\mathrm{He}(\beta, \bar{\nu}){}^6\mathrm{Li}$. The neutrino direction had to be obtained from observation of the ${}^6\mathrm{Li}$ nuclear recoil. Such experiments, after initial difficulties, indicated that Gamow–Teller transitions such as ${}^6\mathrm{He}$ decay involved the axial vector (A) interaction ($C_{\mathrm{GT}} = C_\mathrm{A}$) and Fermi transitions involved the vector (V) type

($C_F = C_V$). Before this conclusion was final, however, these experiments were overtaken by the collapse of the parity-conservation requirement.

This major advance in our understanding of the weak interaction derives from the consideration by Lee and Yang in 1956 of experimental evidence on the decay of charged kaons. In brief, the 3π (τ-mode) and 2π (θ-mode) decay of the K^+-meson indicate identical lifetime ($\approx 10^{-8}$ s) and mass for the parent particle but apparently opposite parity, because of the nature of the 2π and 3π final states. The kaon lifetime indicates that the decay is a weak process, and it is non-leptonic. Lee and Yang suggested that the difficulty could be resolved by the simple but revolutionary assumption that parity is not conserved in a weak decay, and they went on to observe that whereas the validity of parity selection rules seemed well substantiated in electromagnetic and strong interactions, and indeed in the weak interaction as far as the nuclear levels are concerned, nevertheless existing experiments gave no information of this sort for the weak interaction itself. This was essentially because of experimental averaging over spin directions which concealed interference between amplitudes that behaved differently under the parity operation.

The appropriate parity-sensitive experiments were those in which the leptonic decay of a particle or nucleus could be examined with knowledge of the spin axis of the decaying state. The first results were obtained in 1957 for the $\pi \to \mu \to e$ decay and for the Gamow–Teller beta-decay of polarized ^{60}Co. In the former experiment the electron emission from muons was found to be asymmetric with respect to the direction of travel of the muon, and if the muon were assumed to be longitudinally polarized, this would indicate an asymmetry with respect to spin direction. In the ^{60}Co experiment the nuclear spin was aligned by cryogenic techniques and again the angular distribution of the electron emission in the decay was found to have the form $(a + b \cos \theta)$ with respect to the spin axis. Reflection of this asymmetric decay process in a mirror displays a different physical situation (Fig. 10.7), contrary to the symmetry expected if parity were conserved. In both cases the effect is seen by the observation of a *pseudoscalar* quantity which is not invariant in mirror reflection, namely the correlation of a vector (linear momentum of the electron) with an axial vector (angular momentum of the decaying particle). The effect is produced by interference of the amplitudes of opposite symmetry that are permitted if conservation of parity between the initial or final state and the emitted leptons is not required. The consequential effect that electrons emitted from unaligned nuclei should be longitudinally polarized (and muons from pions, as assumed above) was also observed. Similar considerations apply to hyperon decays, e.g. $\Lambda^0 \to p + \pi^-$.

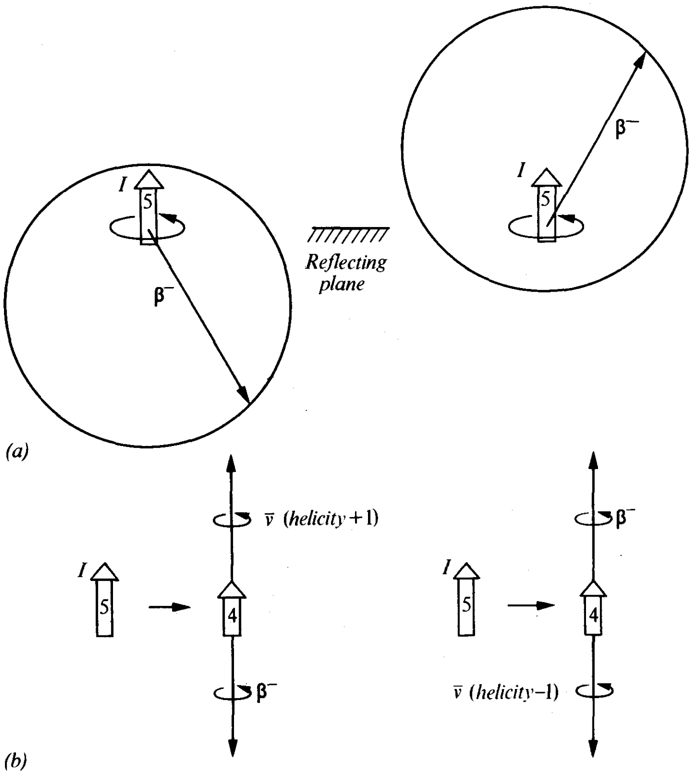

Fig. 10.7 Interpretation of ^{60}Co decay, an allowed Gamow–Teller process. (*a*) Reflection of the nuclear spin (5) and electron momentum in a horizontal mirror; the polar diagram is schematic only. (*b*) Explanation of the asymmetry shown in (*a*) in terms of neutrino theory. In order to change the nuclear spin by $1\hbar$, the spins of the light particles must point along the nuclear axis, but for a prescribed neutrino helicity only *one* of the two mechanisms shown is possible. Experiment indicates the left-hand diagram of (*b*) and hence $\mathscr{H}(\bar{\nu}) = +1$.

The longitudinal-polarization phenomenon, resulting from a pseudoscalar formed from the linear momentum of a particle and its own spin, suggested to Goldhaber, Grodzins and Sunyar (1958) an elegant way of determining the character of the nuclear beta interaction. It was essentially to measure the helicity of the neutrino emitted in the electron-capture process

$$^{152}\mathrm{Eu} + \mathrm{e}^- \rightarrow {}^{152}\mathrm{Sm}^* + \nu_\mathrm{e} \qquad (10.44)$$

The simple nature of this reaction associated this helicity immediately with the circular polarization of the photon from the excited nucleus ^{152}Sm* when it is emitted in a direction opposite to the neutrino. Such photons were selected by imposing a requirement for maximum recoil energy by including a resonant scattering process in the chain of observation and their polarization sense was found by transmission through magnetized iron. The helicity of the neutrino was unambiguously found to be *negative*, i.e. a left-handed screw. Other experiments relating to the longitudinal polarization of the charged particles in beta decays had already been done and in combination with the results of the ^{152}Eu experiment, indicated that the Gamow–Teller interaction was of axial-vector (A) character in agreement with evidence from the electron–neutrino correlation experiments. All 'parity' experiments were also consistent with the conclusions that Fermi-type decays were of vector (V) character and that the antineutrino had positive helicity, as for a right-handed screw. In both cases the helicity was the maximum possible, namely ± 1 for the massless leptons and $\pm v/c$ for electrons or positrons.

The ft-values for transitions in which both the Fermi and Gamow–Teller interactions are effective, and for which the nuclear matrix elements are known, show that for the hadronic term in the matrix element $|C_A/C_V| = |C_{GT}/C_F| = 1{\cdot}23$. From experiments with polarized neutrons, for which the spin axis is known, it further follows that $C_A/C_V = -1{\cdot}23$; the negative sign leads to the common description 'V–A *interaction*'.

10.4.3 The weak matrix element

Following Feynman and Gell-Mann, we now formulate the weak interaction matrix element, using as essential ingredients the non-conservation of parity, the similar strength of all non-strangeness-changing weak interactions, and the observation of left-handed neutrinos.

The matrix element (10.36) is a scalar, whatever the values of the operators. To describe parity non-conservation we need it to contain a pseudoscalar term as well, so that it ceases to be invariant under the parity operation, although it still represents an interaction energy. This is most simply achieved by adding an extra term to the lepton operator which ensures that the neutrino taking part in the weak interaction is left-handed (or right-handed for an antineutrino). Although this apparently ascribes parity non-conservation to the leptonic system it must be remembered that the effect is found also in non-leptonic processes, e.g. (10.5) and is therefore a property of the interaction as well as of the neutrinos. The lepton term then reads

$$\phi_e^* \boldsymbol{O}_x (1+\gamma_5)\phi_\nu \tag{10.45}$$

where γ_5 is a Dirac operator with the required property and $\gamma_5^2 = 1$; this quantity also occurs in the axial-vector operator. It has already been noted that the parity operation applied to such a neutrino leads to a non-physical state.

Introducing now the experimental result that only the V and A interactions are effective in nuclear beta decay and omitting all operators other than γ_5, the matrix element (10.36) can be put in the form (Ref. 1.1a, Appendix B)

$$H_{if} = g \int \psi_f^*(C_V - \gamma_5 C_A)\psi_i \,.\, \phi_e^*(1+\gamma_5)\phi_\nu \, d^3r \qquad (10.46)$$

This shows that if C_V were equal and opposite to C_A the hadron and lepton terms would be exactly equivalent, each invoking left-handed particles. In fact, we have already noted that $C_A = -1{\cdot}23 C_V$, probably because owing to strong interaction effects the nucleons are not strictly Dirac particles, and also because of virtual emission of pions in the axial vector interaction.

It might be thought that strong-interaction effects would be significant in vector processes such as the pure Fermi superallowed beta decays. However, the coupling constant $g_\beta^V = gC_V$ extracted from the *ft*-values for such processes is very close to that derived from the halflife of the muon according to the V–A theory. This agreement has been clarified by Feynman and Gell-Mann in the *conserved vector current (CVC) hypothesis.*

To see how this works, a further analogy is drawn to electromagnetism, in which the interaction of a proton with an electromagnetic field is the same, apart from sign, as that of an electron. The electric charge, in fact, is not *renormalized* by the emission of virtual pions. Now for beta decay, referring back to Fig. 10.1*b*, we may represent the process as a coupling of two particle *currents*, via an intermediate particle exchanged at the vertices. The hadronic current must contain a vector part and an axial-vector part, to account for the observed decays, but these parts are identical in the leptonic current. The CVC hypothesis asserts that the vector part of the hadronic current is *strictly* analogous to the electromagnetic current and is, therefore, free of divergence. Physically, the situation is as shown in Fig. 10.8 and means that although virtual emissions of pions may take place from a nucleon, the emitted pion must itself be capable of beta decay, so that the overall decay probability is unaltered. The predicted decay

$$\pi^+ \to \pi^0 + e^+ + \nu_e \qquad (\Delta I = 0,\ \Delta T = 0) \qquad (10.47)$$

has been observed with the correct basic rate, or $ft_{1/2}$-value, which of course is exactly that of superallowed beta decay. Other detailed consequences of the CVC hypothesis have been verified.

In terms of currents, the general weak interaction can usefully be described by regarding the Hamiltonian energy as due to the

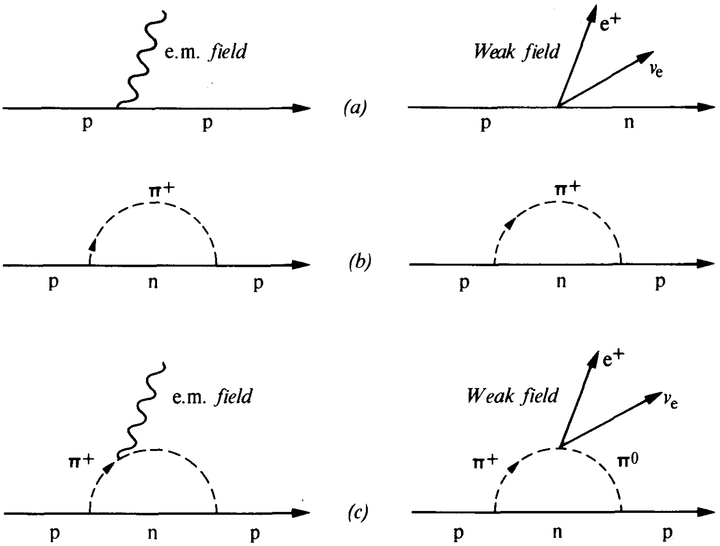

Fig. 10.8 Coupling of a proton to the electromagnetic and weak interaction fields. (*a*) Proton without meson cloud. (*b*) Proton and virtual meson, uncoupled. (*c*) Restoration of coupling by ascribing consequences of charge and weak decay to the pion.

interaction of a current J_W with itself (cf. eqn (9.6) for the electromagnetic interaction). The weak current will contain leptonic parts j_e, j_μ for the creation of electrons or muons, and hadronic parts S and J for strangeness-changing and non-changing processes respectively:

$$J_W = j_e + j_\mu + J + S \tag{10.48}$$

Taking a product of two such currents we obtain terms such as $(j_e J)$ which applies to the nuclear beta decay just discussed, in which J breaks down into the vector and axial vector parts J_V, J_A. Other products describe muon decay and capture and strange-particle processes.

An important modification to this description of the weak interaction was made by Cabibbo, who proposed that the hadronic currents J and S should not be coupled-in equally. This is indeed necessary because strangeness-changing processes are slower than ordinary beta decays by at least a factor of 10 and apparently do not participate in the $\Delta S = 0$ universality. Specifically, Cabibbo wrote

$$J_W = j_e + j_\mu + J \cos \theta_C + S \sin \theta_C \tag{10.49}$$

so that if the coupling constant for muon decay $(j_e j_\mu)$ which involves only the leptonic current is g_μ, then that for vector beta decay $(j_e J_V)$

is $g_\beta^V = g_\mu \cos\theta_C$. The $\Delta S = 1$ leptonic decays of the strange particles $(j_e S, j_\mu S)$ have a coupling constant $g_\mu \sin\theta_C$ and universality is redefined in terms of the Cabibbo angle.

From existing hyperon decay data the Cabibbo angle is found to be

$$\theta_C = \arcsin(0{\cdot}233 \pm 0{\cdot}005) \qquad (10.50)$$

and from the observed muon coupling constant

$$g_\mu = 1{\cdot}4358 \pm 0{\cdot}0001 \times 10^{-62}\ \mathrm{J\,m^3} \qquad (10.51)$$

application of the relation $g_\beta^V = g_\mu \cos\theta_C$ gives

$$g_\beta^V = 1{\cdot}3962 \pm 0{\cdot}0017 \times 10^{-62}\ \mathrm{J\,m^3} \qquad (10.52)$$

The directly observed value of g_β^V is obtained from the pure Fermi superallowed transitions of the mass (4n+2) nuclei ^{14}O, ^{26}Al^m, ^{34}Cl, ^{38}K^m, ^{42}Sc, ^{46}V, ^{50}Mn, ^{54}Co. These decays are between $I^\pi = 0^+$ states and have $T = 1$, $\Delta T = 0$, for which $M_{GT} = 0$ and $M_F = \sqrt{2}$. The $ft_{1/2}$-values, after the introduction of small charge-dependent corrections, are closely similar, in accordance with the CVC hypotheses, and the mean value of 3088 s, inserted in equation (10.29b), gives

$$g_\beta^V = 1{\cdot}4116 \pm 0{\cdot}0008 \times 10^{-62}\ \mathrm{J\,m^3} \qquad (10.53)$$

This differs from the value predicted from g_μ, but is sufficiently close to it to lend support to the CVC theory as modified by Cabibbo, which explains why beta decay is slower than expected from muon decay.

The residual discrepancy between the values (10.52) and (10.53) is almost certainly connected with the fact that certain model-dependent electromagnetic corrections are not included in the present calculation of g_β^V. These bring in not only the postulated exchange particle of the weak interaction but also the structure of the nucleon itself, namely its quark content. Difficulties in these calculations have now largely been removed by the theoretical advances that unify the weak and electromagnetic interactions and by the observation of the non-strangeness-changing neutral currents in neutrino interactions (Sect. 2.2.3) that support these theories (Ref. 2.4). Since the experimental accuracy of the coupling-constant measurements is quite high, the discrepancy may be used either to estimate the mass of the exchange particle or to predict the average charge of the quarks in the nucleon. In an analysis directed to the latter object, Wilkinson (Ref. 10.1) concludes that nuclear beta-decay data are consistent with quark charges of $\frac{2}{3}e$ and $-\frac{1}{3}e$, in agreement with the results of electron and neutrino scattering experiments (Ref. 2.3).

10.5 Summary

The weak interaction regulates the nuclear decays, such as beta decays, that are not dominated by radiative (electromagnetic) or hadronic (strong) processes. Throughout the history of nuclear physics it has been a fertile ground for new concepts. The chapter mentions Pauli's hypothesis of the neutrino, after which Fermi was able to formulate a theory of nuclear beta decay by analogy with radiative processes. The classification of beta-decaying nuclei in terms of Fermi's theory is described. No detailed formulation of the weak interaction matrix element can be given, since the interaction is not known, but it is constrained by relativistic invariance principles. Since 1957 it has been known also that it contains terms which interfere in such a way that parity is not conserved in weak processes. The experimental evidence for this discovery is outlined. The strength of the weak interaction is directly measurable by beta-decay experiments among which the vector-type Fermi decays have a special significance. It is shown that their decay rate may be related to that of the (structureless) muon if a parameter determined by strange-particle leptonic decay rates is introduced. Even more fundamentally, there is promise of a unification of the weak and electromagnetic interactions, at least at high energies.

Examples 10

10.1 The atomic mass of ^{137}Ba is given by $(M-A)=-87\,734$ keV. Assuming the decay scheme shown in Fig. 10.2 calculate the $(M-A)$ value for ^{137}Cs given that the electron kinetic energy at the upper limit of the main beta spectrum is 514 keV, and that the radiative transition energy is 661·6 keV. [−86 558 keV]

10.2 The atomic masses of $^{74}_{32}$Ge, $^{74}_{33}$As and $^{74}_{34}$Se are 73·921 18, 73·923 93 and 73·922 48. Calculate the Q-values for the possible decay schemes linking these nuclei. [$Q_{\beta^-}=1{\cdot}35$, $Q_{\beta^+}=1{\cdot}54$, $Q_{\rm EC}=2{\cdot}56$ MeV].

10.3* Show that the relativistic expression for the ratio of nuclear recoil energy to maximum electron energy in β^--decay is $T_R/T_e=(Q+2m_e)/(Q+2M_R)$ where Q is the energy available for the decay products and M_R is the mass of the recoil nucleus.

Evaluate T_R for the ^{137}Cs case, Example 10.1. [0·003 keV]

10.4 Use the result of Example 10.3 to infer the nuclear recoil energy in the case of electron capture, releasing energy $Q_{\rm EC}$. Assume that the neutrino mass is zero.

For the decay $^{37}{\rm A}\rightarrow{}^{37}{\rm Cl}$, $Q_{\rm EC}=0{\cdot}82$ MeV and $T_R=9{\cdot}7\pm0{\cdot}8$ Ev. Show that these figures are consistent with $m_\nu=0$.

10.5 The reaction ^{34}S(p, n)^{34}Cl has a threshold at a laboratory proton energy of 6·45 MeV. Calculate non-relativistically the upper limit of the positron spectrum of ^{34}Cl assuming $m_ec^2=0{\cdot}51$ MeV, $M_n-M_H=0{\cdot}78$ MeV. [4·47 MeV] (See Ex. 1.25 for the relativistic correction)

10.6 Write down the phase-space part of expression (10.16), in terms of the variables W and p for the electron (upper limit $=W_0$) and obtain the quantity $N(p)={\rm d}\lambda/{\rm d}p$ *without* the assumption of zero neutrino mass.

By examination of the variation of $N(p)$ with p near the upper limit, verify the dependence on neutrino mass shown in Fig. 10.4. (Assume for this purpose that the main variation near W_0 is due to the neutrino momentum, given by $p_\nu^2 \propto (W_0 - W)$ for non-relativistic motion.)

Compute and plot the momentum spectrum (*a*) for $m_\nu = 0$, and (*b*) for $m_\nu = nm_e$. Compute and plot also the energy spectrum $d\lambda/dW$ given by equation (10.16) for the same two cases and verify that the spectrum is symmetrical for $m_\nu = m_e$.

10.7 In a very low-energy β-spectrum (e.g. ^{14}C with maximum kinetic energy $T_0 = 0{\cdot}156$ MeV), the energy distribution may be approximated by $d\lambda \propto T^{1/2}(T_0 - T)^2\, dT$.

Show that in this case the mean kinetic energy of the spectrum is one-third of the minimum energy.

10.8* In a high-energy β-spectrum, with the maximum energy $E_0 \gg m_e c^2$, show that the decay constant λ is approximately proportional to E_0^5.

10.9 In a typical experiment to determine the β^--spectrum of ^{137}Cs, the following relative counting rates were observed at the indicated $B\rho$-values in a magnetic spectrometer

$B\rho$ (tesla m $\times 10^6$)	1370	1780	2230	2640	2866	2960	3080
Relative counting rate	726	855	760	305	152	40	30

Allowing for the momentum dependence of the spectrometer acceptance, make a Fermi–Kurie plot of these data, interpolating values of the function $p^2F(Z, p)$ from the following table

$p = p_e/m_e c$	0·6	0·8	1·0	1·2	1·4	1·6	1·7	1·8	1·9
$p^2F(Z, p)$	2·0	2·9	3·9	5·1	6·5	8·0	8·9	9·7	10·6

Deduce the end-point energy of the spectrum on the (incorrect) assumption that it has an allowed shape.

10.10* Show that the maximum total electron energy E_0 in the decay of a muon at rest is

$$E_0 = \tfrac{1}{2} m_\mu c^2 \left[1 + \left(\frac{m_e}{m_\mu}\right)^2\right]$$

10.11* The maximum positron energy in the decay of ^{34}Cl ($t_{1/2} = 1{\cdot}57$ s) is 4·47 MeV and the Fermi factor $F(Z, p)$ is equal to 0·71 over most of the spectrum.

Evaluate the integrated Fermi function $f(Z, p_0)$ and the comparative halflife.

10.12* On the assumption that the nuclear matrix element for the ^{34}Cl decay is given by $|M_F|^2 = 2$ and $|M_{GT}|^2 = 0$, obtain the weak interaction coupling constant g_β $(= g_V)$.

10.13 Use equation (10.25) to predict the decay rate by K-electron capture in the case of $^{34}_{17}Cl$, for which data are given in Example 10.11. [$3 \times 10^{-4}\ s^{-1}$]

10.14 Repeat the calculation of Example 10.13 for the case of muon capture by $^{34}_{16}S$ under the simplest possible assumptions. [$\approx 10^7\ s^{-1}$]

10.15 The value of the weak interaction coupling constant is $g = 1{\cdot}44 \times 10^{-62}$ J m^3. Show that in natural units, with $\hbar = c = 1$, it has the value $G = 10^{-5}/m_p^2$ where m_p is the proton mass.